PROGRESS IN ORGANIC COATINGS (ISSN: 0300-9440) 77(7): 1226-1232 (2014).

DOI: 10.1016/j.porgcoat.2014.02.007

One-pot synthesis of gelatin-based, slow-release polymer microparticles containing silver nanoparticles and their application in anti-fouling paint

Tamás Szabó[a]*, Judith Mihály[b], István Sajó[c], Judit Telegdi[a, d], Lajos Nyikos[a]

[a]Department of Interfaces and Surface Modification, Institute of Materials and Environmental Chemistry
[b]Department of Biological Nanochemistry, Institute of Molecular Pharmacology
[c]Department of Functional and Structural Materials, Institute of Materials and Environmental Chemistry
[a,b,c]Research Centre for Natural Sciences, Hungarian Academy of Sciences, Pusztaszeri street 59-67., Budapest, H-1025 Hungary
[d]Óbuda University, Rejtő Sándor Faculty of Light Industry and Environmental Engineer, Institute of Media-technology and Light Industry; Doberdó út 6. Budapest, H-1034 Hungary
*corresponding author, e-mail: szabo.84.tamas@ttk.mta.hu, tel.: +36 1 438-1100 / 545

Abstract

Gelatinous polymer matrix microparticles containing silver nanoparticles (AgNPs) were prepared by a novel method to obtain quasi non-swelling anti-fouling paint additives with slow-release characteristics. A w/o type dispersion were elaborated with the aqueous phase of gelatin, urea, silver-nitrate and formaldehyde dispersed in linseed oil. Gelatin was cross-linked by formaldehyde, together with urea for limiting the swelling of the product. Silver-nitrate was reduced with the assistance of gelatin and formaldehyde into homogenously dispersed AgNPs. The microparticles and embedded AgNPs were visualized by scanning and transmission electronmicroscopy. Encapsulated AgNPs with ~18nm crystallite size were identified by X-ray powder diffraction. Characterization of gelatin-urea-formaldehyde polymer matrices was carried out by attenuated total reflectance FTIR spectroscopy. Silver dissolution from microparticles and paints with AgNP-containing microparticles was measured by inductively coupled plasma spectrometer and resulted in highly sustained release, compared to unmodified gelatin microparticles and paints containing uncapsulated silver salts. A seven month-long fouling experiment run in natural sweetwater media showed that solvent-based acrylic paint with AgNPs-containing gelatinous microparticles as additives offered resistance against biofouling at low Ag-release ratio.

Keywords

silver nanoparticle, gelatin microparticle, slow-release, anti-fouling, encapsulation

1. Introduction

After centuries of questionable and not reliable usage, during the last few decades silver is about to be involved into scientific fields of antibacterial, biocidal applications. Biocide effect of silver which is assigned to its ionic and metallic nanoparticle form (herein AgNP) either, is expressed against certain lifeforms due to catalytic oxidative reactivity, disruption of electron transfer, prevention of DNA unwinding, etc. [1].

Today AgNPs or Ag+ ions as biocide agent are being investigated for numerous applications like water filter membranes [1], fabrics [2-5] thin layers [6-9], anti-fouling thick coatings [10-14,], dental materials and devices [15,16], surface modified implants [17-21], catheters and bone cements [22]. In the surgery they have major role as disinfectants in burn wound dressings [23-25].
AgNPs immobilized in certain biopolymeric carrier structures are quite in sight of interest in the last decade. AgNPs are embedded in- or fixed on the surfaces of hydrogel beads [26,27] or fibers [28,29] of nano/micron range. General criteria towards them is the homogenous distribution of AgNPs in the polymer matrix or on the surface and the accessibility for aqueous media.
General incidence of biopolymers in nature, low cost, biocompatibility, biodegradibility makes biomaterials apparent to use as host material for AgNPs. Biopolymers such as peptide-based (gelatin [28,30-35], glutathione [36], keratin [37]) or polysaccharyde-based (alginate [26,27,38-41], chitosan [32,34,42-47], starch [48]) polymers are good capping agents for silver ions [38,49,50]. Amine groups, oxygen atoms present in ring or –OH groups stabilize Ag^+s via complexation and ensure homogenous distribution of later reduced AgNPs within the polymer solution or matrix. Biopolymer-driven reduction of metal ions into stabilized AgNPs without further reducing agents are also being investigated [28,51,52].
The preparation methods of AgNPs in micro/nano-biopolymers consist of four major steps in various order depending on their purpose. The steps are the following: polymer shaping (fibers: spinning/extrusion, microspheres:mostly emulsification in w/o systems); cross-linking polymeric chains (precipitation in another liquid phase (e.g. alginates) or with linking agents (e.g. aldehydes); silver incorporation into polymer (swelling in Ag^+-containing solution); silver ion reduction to metallic AgNPs. Depending on the circumstances, the mentioned steps might be changed or combined. Combination of polymer shaping and silver incorporation (Ag^+ or Ag^0) is general, it is followed by reduction and cross-linking. It is even usual that silver incorporation follows the shaping and cross-linking of host polymer.
In this paper we extend the preparation and characterization of our former work [53] presenting in details the one-pot synthesis of AgNPs-containing gelatin-urea microparticles cross-linked with formaldehyde (herein AgNPs@GMP) as well as their application in solvent-based anti-fouling paint.
The aim of our work was to prepare hydrophilic polymer particles of 10-20μm diameter with the ability of releasing ionic silver into aqueous media. As we tend to use the particles as additives for underwater paints or coatings, their diameter is limited to the mentioned size. The polymer particles should contain homogenously distributed AgNPs embedded without higher agglomeration. The last criteria was that the hydrophylic microparticles should not swell significantly in aqueous neither in organic media. Swelling of the microparticles may cause inner strains in the applied coating which leads to desintegration. Indifferency towards organic solvents is also important because the particles would be stored in solvent-based ship paints.
In order to fulfill all these criteria we have realized a one-step process in which the reduction of Ag^+ ions and the polymer cross-linking run parallelly in time. To reduce the swelling of gelatin (which could happen even in cross-linked form) we co-polymerized it with an other biocompatible material, urea. The method was water-in-oil dispersion polymerization where the aqueous phase contained the matrix materials (gelatin, urea), the silver source (silver-nitrate) and the cross-linking+reducing agent (formaldehyde).

2. Experimental

2.1. Materials

2.1.1. Chemicals used for preparation of microparticles and coatings
Urea (Fluka, p.a.); gelatin (Reanal, purum); formaldehyde (Sigma-Aldrich, purum, 37% aqueous sol.); silver-nitrate (Reanal, a.r.); silver-carbonate (Reanal, puriss.); linseed oil (Aldrich, purum); toluene (Carlo Erba, a.r.); anti-fouling paint without commercial anti-foulant: dry matter ~50% acrylate resin, solvents: isobutyl acetate 3-12% and methoxypropyl acetate 20-45% (Dunaplast Anti-fouling from Dunaplast Ltd., 'DPL'); natural sweetwater from Lake Balaton.

2.1.2. Chemicals used at sampling
Sample preparation for inductively coupled plasma spectrometer (ICP) measurements: nitric acid 65% (Spektrum 3D, a.r.), hydrogene-peroxyde 30% (Molar Chemicals Ltd., a.r.); solvent mixture as paint model: isobutyl acetate- methoxypropyl acetate at a mass ratio of 6:40; biofilm fixation: ethanol (Molar Chemicals Ltd., a.r.); biofilm visualization: 0,01% acridine orange in ethanol.

2.2. Preparation of AgNPs@GMPs

The dispersion polymerization method (Scheme 1), was based on our previous work [53]: in 15mL distilled water 2.0g gelatin, 3.0g urea, 0.45g silver-nitrate were dissolved at 40°C and then 11.21g formaldehyde solution (in excess) was added with stirring. Afterwards this aqueous solution was poured into 65mL linseed oil and stirred at 1000rpm with magnetic stirrer. The obtained emulsion was heated to 85°C with 1C°/min heating speed and kept stirred for 5 hours. In one hour the colour of the emulsion turned into dark brown. The microbeads were left to settle for a few minutes, then were cleaned from oil via decantation with toluene, finally dried under IR light and ground.
Two reference samples were produced. One without urea and formaldehyde and another without silver-nitrate. All other circumstances were constant.

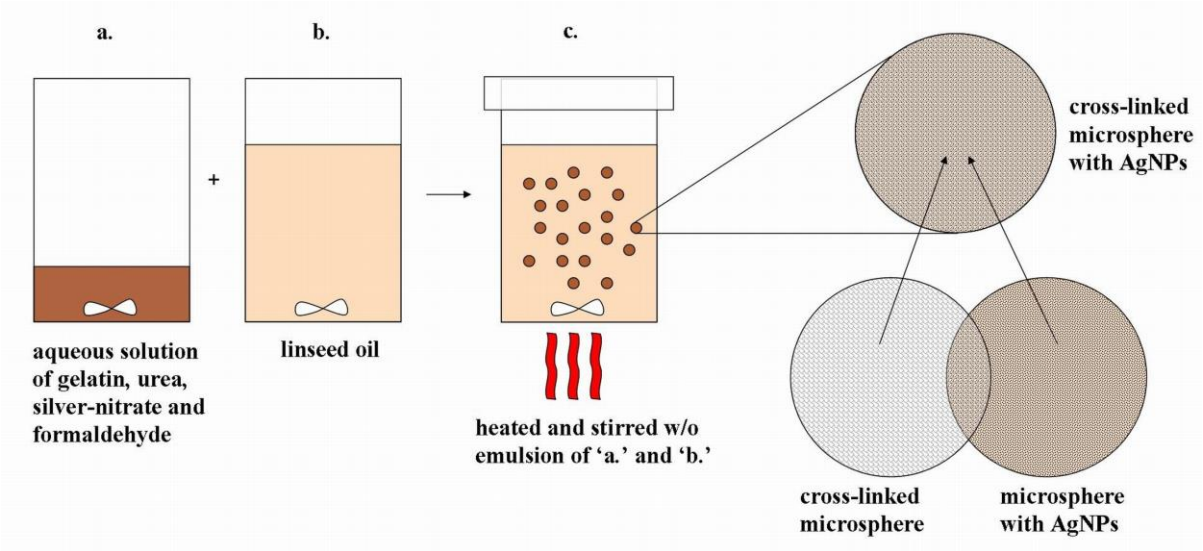

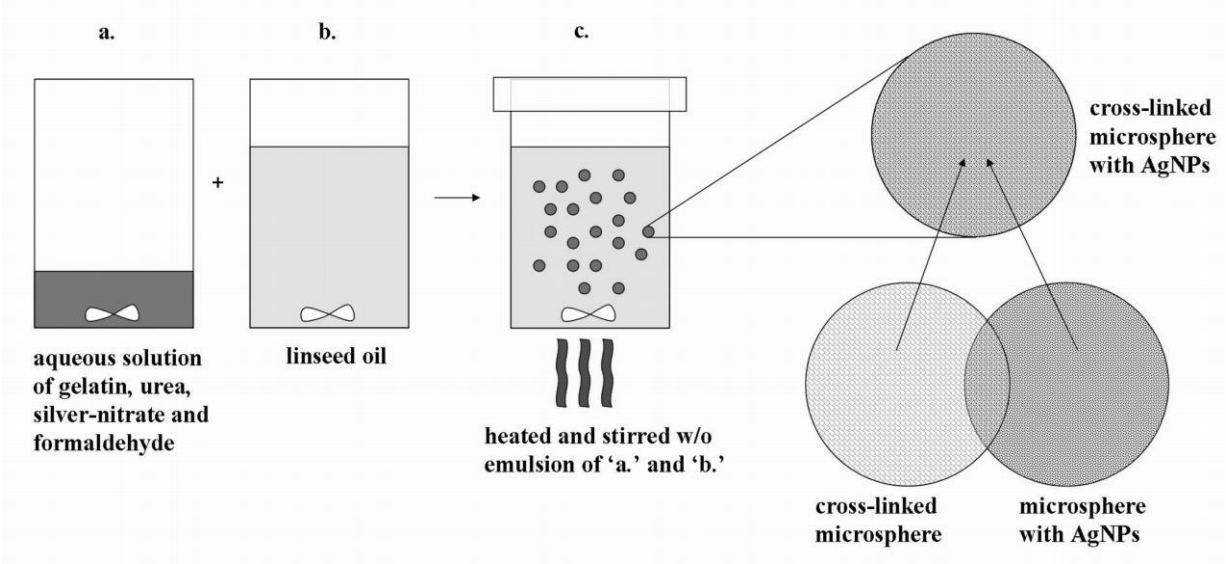

Scheme 1. Preparation scheme of AgNPs-containing gelatin-urea-formaldehyde microparticles.
>>Scheme 1., size: 1.5 column; color on the web, greyscale in print<<

2.3. Preparation of paint samples

2.3.1. Preparation of paint samples for anti-fouling efficiency test
AgNPs@GMPs were mixed into 'DPL' in 4.23 w/w%. The paint was applied on glass surfaces then dried for 2 days. Two reference series were prepared: 'DPL' with 0.2 w/w% silver-carbonate (0.16 w/w% Ag), and 'DPL' without any additives.

2.3.2. Preparation of paint samples for Ag^+ dissolution test
Samples for monitoring Ag^+ dissolution were prepared by adding AgNPs@GMP to 'DPL' paint. The concentration was 4.23 w/w% for microparticles (and 0.16 w/w% for Ag because the Ag content of microparticles is 3.55 w/w%) based on fouling test in which this composition showed excellent efficiency in preliminary experiments. The as prepared paints were applied on 5x5x5mm polymeric foam cubes to enlarge the surface of the coating. For comparison two other silver-containing coating were obtained: one with silver-nitrate (0.252 w/w%) and an other with silver-carbonate (0.2 w/w%). Both had the same concetration of Ag as the microparticle-containing coating (0.16 w/w%). The coated surfaces were dried for 2 days under room temperature airstream until no weight-loss was measured.

2.4. Characterization methods and equipments

2.4.1. Size, size distribution and chemical structure of microparticles
The size and size-distribution of the AgNPs@GMPs were visualized by scanning electron microscope (Zeiss EVO 40 XVP, SEM) as well as by optical microscope (Zeiss Axio Imager A1, OM). Samples for electronmicroscopy were sputter-coated with gold.
Fourier-transform infrared (FTIR) spectroscopy was applied in determination of the chemical composition of the microparticles with or without cross-link and AgNPs.
FTIR spectra were recorded using attenuated total reflection (ATR) technique by means of a Varian 2000 (Scimitar Series) FTIR spectrometer (Varian Ltd, USA) equipped with nitrogen cooled MCT (mercury-cadmium telluride) detector and adjusted with a 'Golden Gate' (Specac Inc, UK) single reflection diamond ATR unit. Spectra were collected by co-addition

of 128 individual interferograms with a spectral resolution of 4 cm^{-1}. Each spectrum was ATR corrected using the Varian Resolutions Pro 4.0 software package.

2.4.2. Determination of active component in microparticles

Determiantion of overall silver content of microparticles was carried out with inductively coupled plasma spectrometer (Jobin Yvon 'Emission' JY 138 ULTRACE sequential, ICP) after dissolving and oxidizing the samlpes in boiling cc. nitric acid and hydrogene-peroxide (in 65% HNO_3 at 190°C for 3hrs then cooling down to 100°C and addition of H_2O_2, finally heated up to 180°C for 1hr).

The microparticles with silver were visualized by transmission electronmicroscopy (Fei Morgagni 268D 100 keV, TEM). To make it easier to observe the inner content of the microparticles with TEM, they were embedded into two-component sample-fixing epoxi resin, then were sectioned into 100nm-thick slices with microtome (Leica EM UC6 Ultramicrotome). To obtain the smallest possible thickness, these slices had to be weakened with argon ion beam thinner (Ion Beam Thinning Unit type: IV 4/F/L, Technoorg Linda Scientific Technical Development Ltd. Co.).

In order to determine the oxidation state of the nanoparticles shown by TEM, X-ray diffraction measurements were involved. X-ray powder diffraction (XRPD) patterns were obtained in a Philips model PW 3710 based PW 1050 Bragg-Brentano parafocusing goniometer using CuKα radiation (λ= 0.15418 nm, 40 kV, 35 mA), graphite monochromator and proportional counter. The XRD scans were digitally recorded with a stepsize of 0.04° in the 2θ range of 10 to 85°.

2.4.3. Swelling of microspheres in water and solvent mixture

The swelling ratio of AgNPs@GMPs could not be measured by weighing the water uptake as it was comparable with the mass of moisture absorbed onto the surface of microparticles. That is why an optical microscope with built-in camera was chosen to record the volumetric swelling of both the cross-linked and not cross-linked gelatinous microparticles during 24 hours of leaching. Distilled water and model organic solvent mixture was applied as swelling media.

2.4.4. Release of silver and organic residues from microparticles into water and organic solvent mixture

2.4.4.1. Silver and organic compound release in aqueous media

0.5g of the microparticles were suspended in 200mL distilled water and were stirred 1hr/day at room-temperature. 5mL samples were taken and acidified with nitric acid to dissolve silver nanoparticles or salts. Ag-content was measured by ICP. FTIR-ATR method was used to investigate the dissolution of any organic residues from the microparticles.

2.4.4.2. Dissolution in organic solvent

This investigation was carried out similarly to the aqueous experiments but here the media was isobutyl acetate and methoxypropyl acetate mixture, used as paint model. In this case FTIR-ATR method was also appropriate to detect organic residues.

2.4.5. Silver dissolution from paint into water

Equal amounts of the three painted foam samples were put in 600mL room-temperature distilled water. The mixture was stirred only for a short time per day.. During two months water were taken out in 10mL aliquots and nitric acid was added to dissolve water-insoluble silver salts if there were any. The silver ion dissolutions were followed by ICP.

2.4.6. Anti-fouling effectiveness

Anti-fouling effect was followed during an informative adhesion test. Glass slides coated with 'DPL' (see under *2.3.1.*) were dipped into 2-2L natural lake water and the containers were held at room conditions. The monitoring lasted 7 months, this was a much longer test period than reported earlier [53]. The growth of biofilm as a function of time is represented. At sampling, the panels were dried and organisms adhered on the surface were stained with acridine orange solution and were photographed through optical microscope in fluorescence mode. Images of adhered biolayers were evaluated by Axio Vision rel. 4.6.3. software.

3. Results and Discussion

3.1. Size and morphology of microparticles

Based on SEM micrograph, average diameter of the AgNPs@GMPs is between 10 and 20 microns, represented by Fig. 1. Though during emulsification step no surfactants were used, the viscous linseed oil helped to obtain the proper particle size and size distribution. The polyhedral surface of the particles can be originated to their pre-drying state: after separation from linseed oil the microparticles still contain water, they are soft and deform each other. During the drying process, the particles physically adhere to each other but can be separated easily by grinding. The result is a fine brown powder of compact microparticles (Fig. 2).

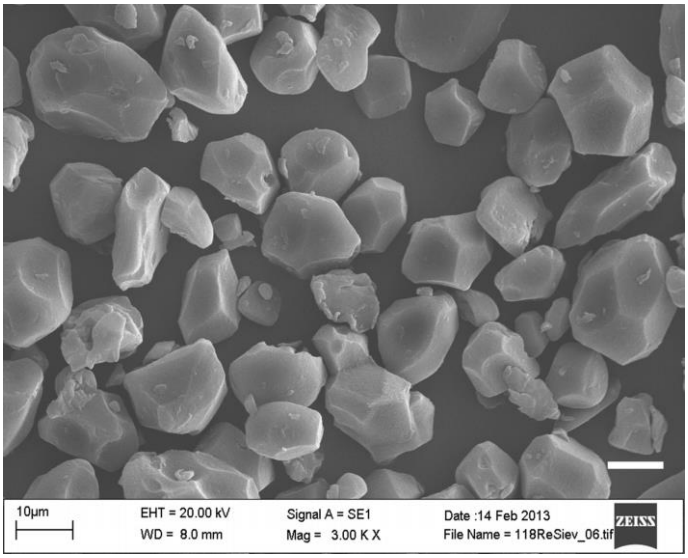

Fig. 1. SEM micrograph of AgNPs@GMPs. The white scale bar represents 10µm.
>>Fig. 1., size: 1.0 column, greyscale on the web, greyscale in print<<

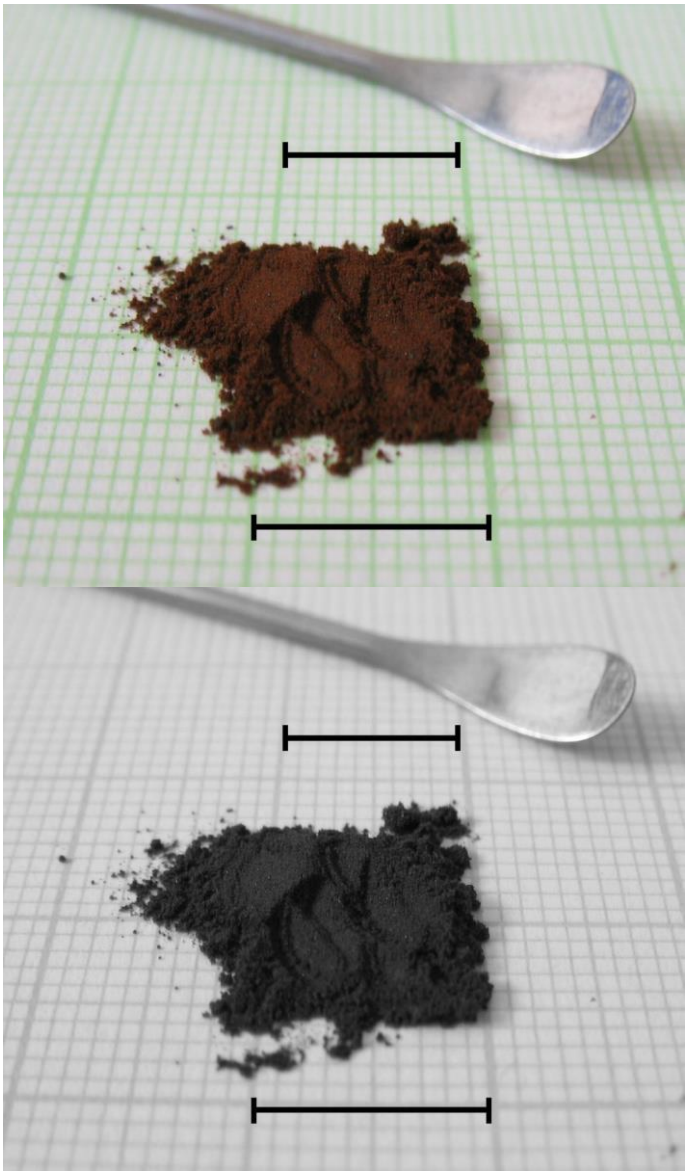

Fig. 2. Fine brown powder of microparticles containing AgNPs after drying and grinding. The black bars represent 10mm.
>>Fig. 2., size: 1.0 column; color on the web, greyscale in print<<

3.2. Chemical structure of microparticles

The FTIR-ATR spectrum of gelatin (Fig. 3,A) shows characteristic absorption bands of natural proteins [54]: around 3300 cm^{-1} the broad band, named also Amide A band, belongs to –N-H stretching band of peptide linkage in proteins, overlapped with the broad H-bonded OH stretching. The two other very specific bands are the Amide I and Amide II bands, at 1648 and 1635 cm^{-1}, respectively. The former is composed mainly of C=O stretching (around 80%), the later originates from the -NH_2 bending (40-60%) and the C-N stretching (20-40%) of amide groups. The Amide III band of medium/weak intensity at 1239 cm^{-1} is assigned as N-H deformation.
After cross-linking reaction with formaldehyde and urea (Fig 3, B), slight spectral changes can be observed. The bands at 2939, 2862 cm^{-1} and 1735 cm^{-1} (belonging to stretchings of CH_2 and C=O groups, respectively) are due to linseed oil impurities used as reaction medium. In the Amide A region, the shape of the broad band is changed; the band envelop maxima is shifted for higher wavenumber (from 3285 cm^{-1} to 3293 cm^{-1}) and a new shoulder at 3366 cm^{-}

[1] appears. These changes indicate that the –N-H, -O-H bonding structure of the gelatin is affected by the cross-linking reaction. As to the Amide I band at 1630 cm^{-1}, no changes was witnessed suggesting that the carbonyl moiety of the peptide linkages are not involved in the cross-linking reaction. At the same time an increase in intensity and a shift at Amide II was observed indicating as well that mainly -NH_2 groups are participating in cross-linking reaction (probably by a Schiff-base related reaction mechanism) [55]. The spectral features between 1500-1200 cm^{-1} indicates a higher number of CH_2 groups compared to 'pure' gelatin, as presented also by the medium intense CH_2 rocking band at 1249 cm^{-1}. The bands around 1375, 1172, and 1002 cm^{-1} can be assigned as C-H deformation of CH_2OH, C-O-C stretching and C-O stretching of CH_2OH moieties, respectively, indicating that not all –OH groups of (tri)methylol urea formed by condensation of urea with formaldehyde are participating in cross-linking of gelatin. (The absence of the strong C=O vibration of urea-derivates from all the cross-linked gelatin spectra could be explained by the fact that due to the strong H-bonding network they should be down-shifted to lower wavenumbers and overlapped with the Amide II band.)

When the cross-linking reaction was carried out in the presence of Ag-salt (AgNPs@GMPs), the spectrum (Fig. 3, C) resembles much more to the spectrum of condensed urea-formaldehyde (Fig. 3, D), suggesting that the Ag^+ blocks some of the -NH groups (primary silver binding sites) of gelatin active in the cross-linking reaction.

As to the spectrum of gelatin added with Ag-salt (Fig. 3, E), no differences were detected compared to the one of 'pure' gelatin. All the above observations suggest that the presence of Ag+ plays a role in cross-linking reaction of gelatin with formaldehyde and urea.

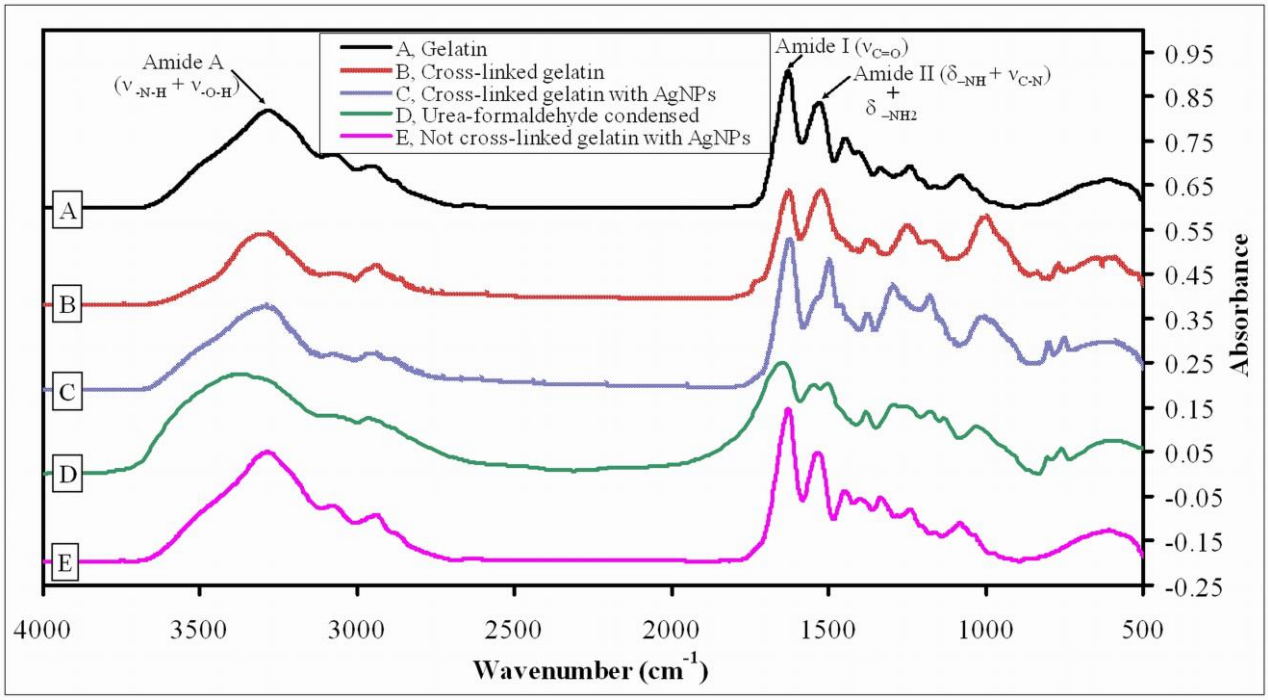

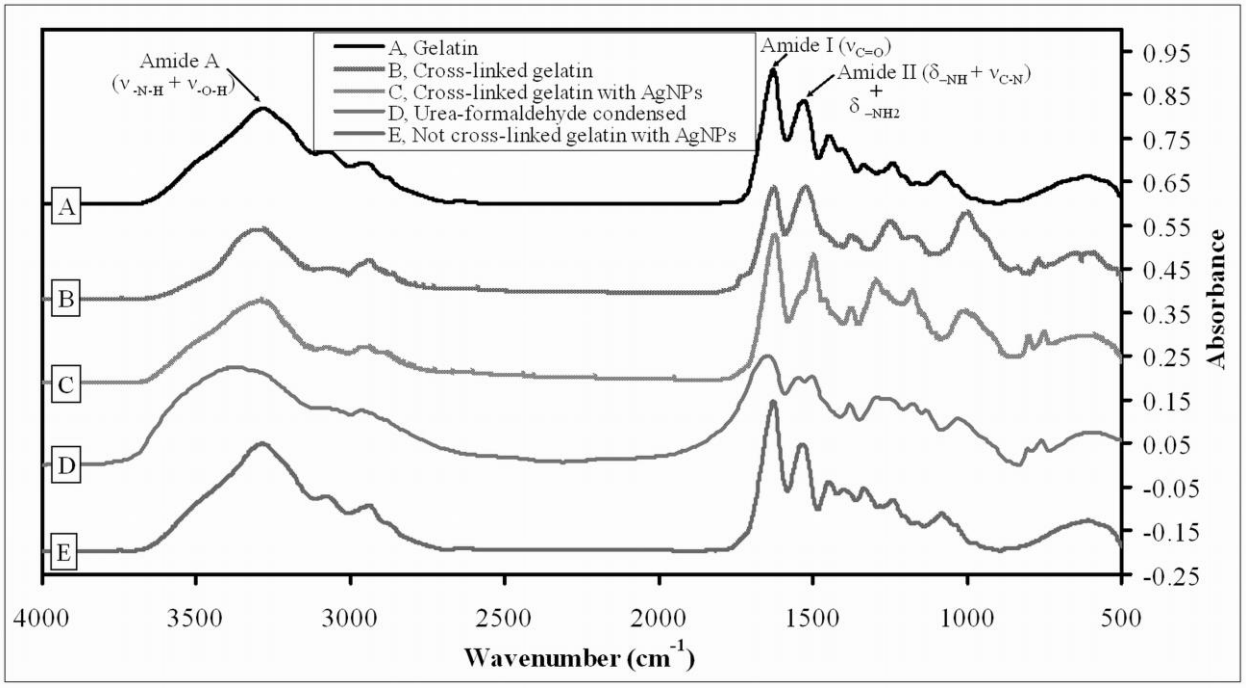

Fig. 3. ATR FT-IR spectra of gelatin (A), cross-linked gelatin recorded without, and with AgNPs, (B) and (C), respectively and gelatin with AgNPs (E). Spectrum of condensed urea-formaldehyde polymer (D) is also present.
>>Fig. 3., size: 1.5 column; color on the web, greyscale in print<<

3.3. Active agent content in microparticles

The overall silver content of cross-linked (AgNPs@GMPs) and not cross-linked polymer microparticles were 3.55 w/w%, yielded by ICP measurements.
By TEM visualization the Ag-content can be seen on Fig. 4A and Fig. 4B. The images of the Ar^+ ion beam-thinned, sliced polymer microsphere layers show the homogenously dispersed silver nanoparticles in them. Due to the relatively small concentration of metallic particles in polymer matrix, electron-diffraction pattern was not possible to record.

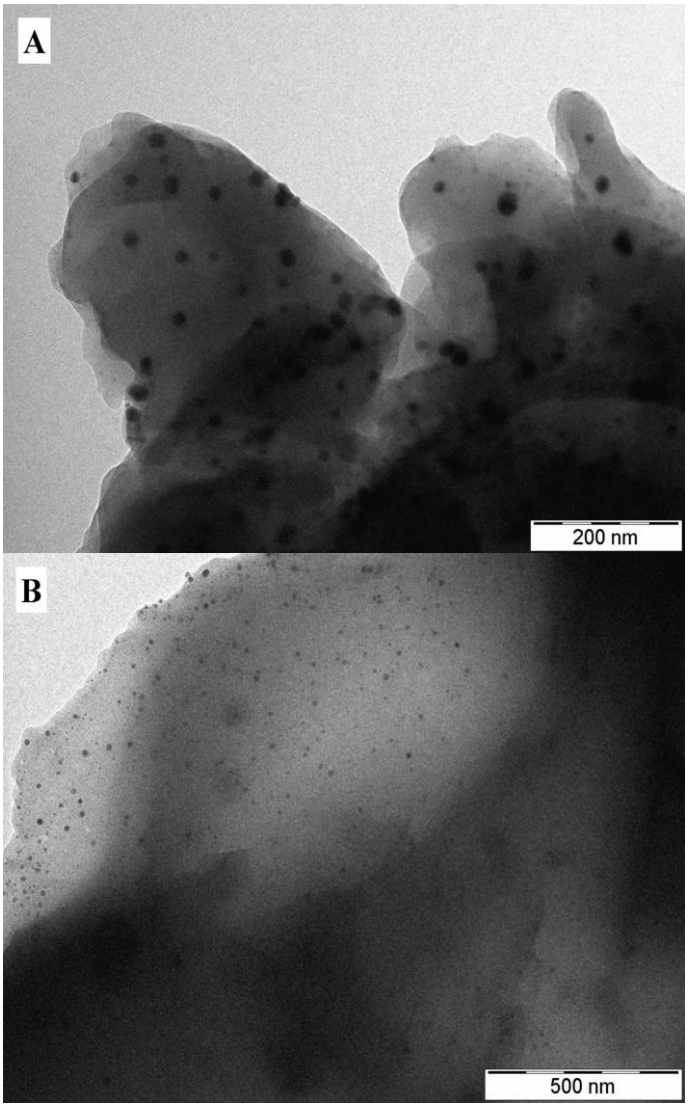

Fig. 4.A-B TEM micrographs of sliced and ion-beam thinned microparticles containing AgNPs with diameter of ~20nm (A), homogenously dispersed in the modified gelatinous matrix (B).
>>Fig. 4.A-B, size: 1.0 column; greyscale on the web, greyscale in print<<

Results of powder XRD measurements on AgNPs@GMPs are shown in Fig. 5. In our experiments AgNPs were formed relying on major characteristic peaks of cubic Ag4f (metallic form) found at 38.150°, 44.317°, 64.487°, 77.550° on 2θ scale referring to the crystal planes (111), (200), (220) and (311) respectively.
Further characteristic peaks were found at 32.271°, 46.274°, 54.878°, 57.532°, 67.535°, 74.544°and 76.810° with lower intesity, corresponding to chlorargyrite (cubic AgCl) crystal planes (200), (220), (311), (222), (400), (331) and (420) respectively. Chlorargyrite formed due to the presence of chlorine contamination. Average size of AgNPs and AgCl were 18nm and 52nm, respectively. The weight ratio of AgCl to overall Ag content is small, 4.8%.

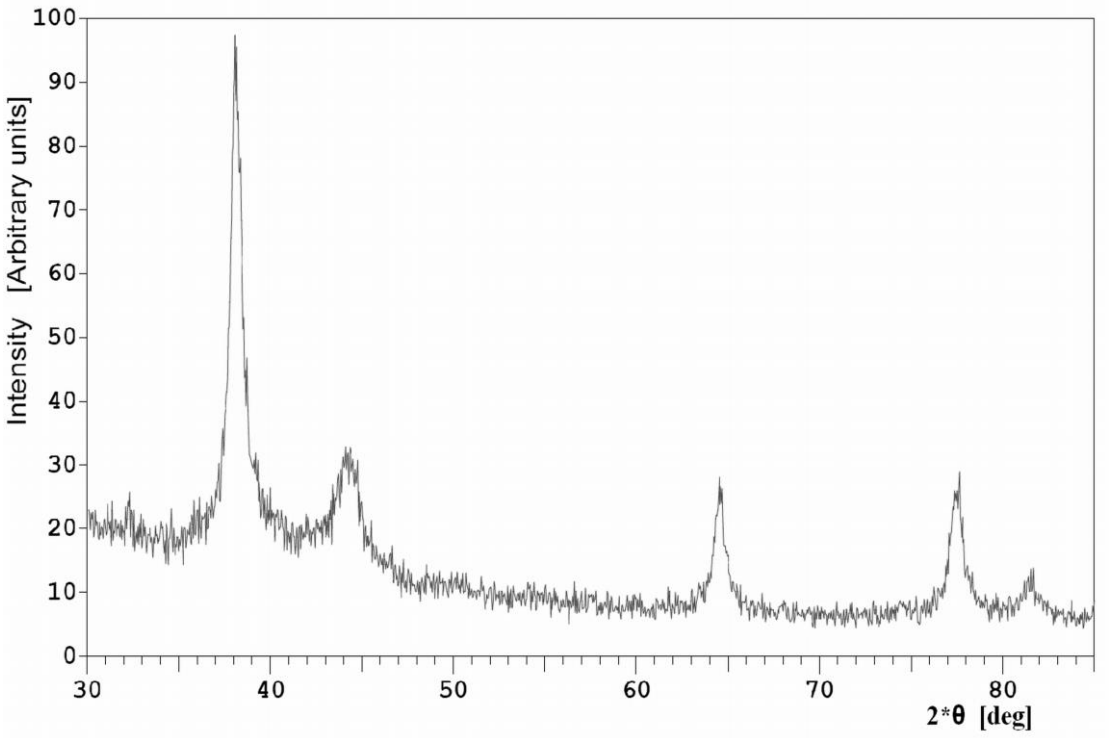

Fig. 5. Powder XRD pattern of gelatin-urea-formaldehyde cross-linked microspheres containing AgNPs and AgCl.
>>Fig. 5., size: 1.0 column; greyscale on the web, greyscale in print<<

3.4. Swelling of microparticles in water and solvent mixture

The swelling of AgNPs@GMPs in water and paint solvent mixture of isobutyl acetate and methoxypropyl acetate was negligible, about 0.5% in diameter. Without cross-linking the microparticles behaved similarly to cross-linked ones in apolar media with negligible swelling but they showed 40% swelling in water in 24 hours.

3.5. Dissolution of silver and organic residues from microparticles in water and organic solvent mixture

In paint solvent mixture there were no traces of silver and unreacted monomers or other organic compounds, confirmed by ICP and FTIR spectroscopic measurements.Therefore no components of AgNPs@GMPs would be released when stored in the paint. Furthermore organic compounds were not present in aqueos media either. On Fig. 6 the released ratio of encapsulated silver can be followed along the nearly one month experiment carried out in water. The results show that cross-linked microparticles allow one magnitude slower Ag^+ release into aqueous media than not crosslinked ones.

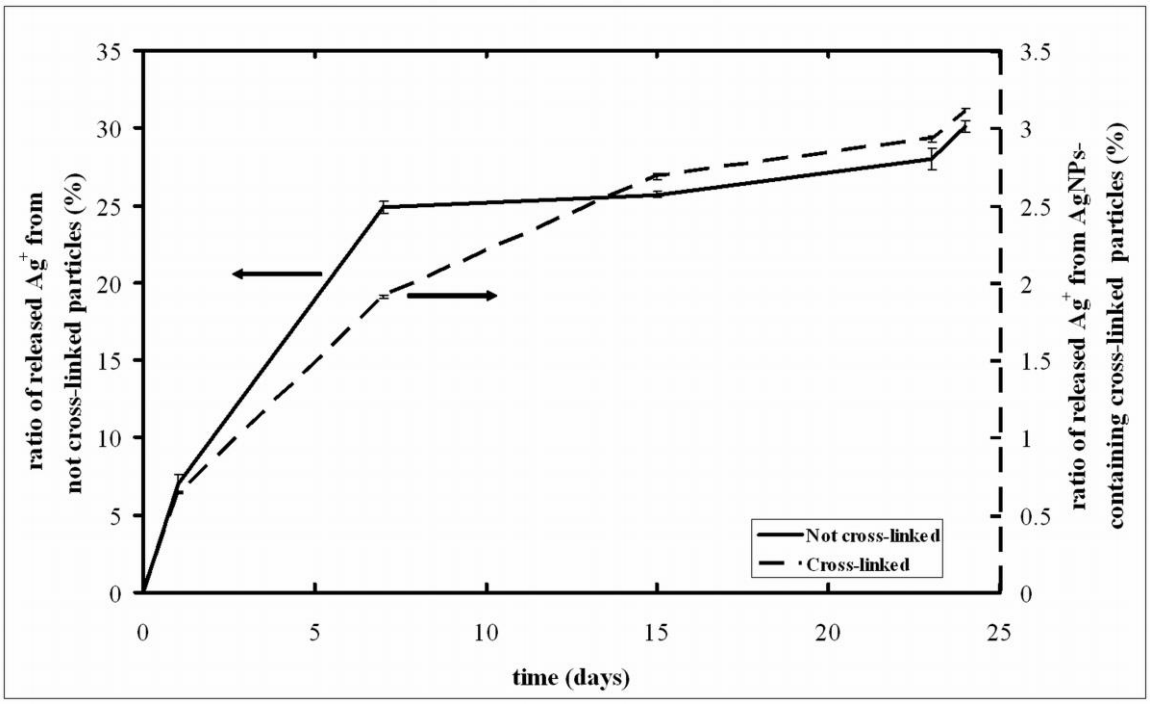

Fig. 6. Ratio (%) of released Ag^+ to the total Ag content of different microspheres, as a function of time. Left and right 'y' axis refers to unmodified (continuous line) and cross-linked (dashed line) gelatin microspheres (AgNPs@GMP), respectively.
>>Fig. 6., size: 1.0 column; greyscale on the web, greyscale in print<<

3.6. Silver dissolution from paint into water

Fig. 7 summarizes a two-month-long observation performed on Ag^+-release from three different paint samples, doped with $AgNO_3$, Ag_2CO_3 and AgNPs@GMPs, respectively. Released quantites are referred to the total Ag-content of the paints. $AgNO_3$ a water-soluble source provided the fastest release rate: in ten days this sample lost ~80% of its total silver content and further it didn't change significantly. Water insoluble Ag_2CO_3 showed slower and more linear profile with an end-point around 40% of its total silver content. Paint with AgNPs@GMPs had the slowest release rate, the diagram runs parallel to the carbonate curve but with values of two orders of magnitude lower, and by the end of the experiment the Ag^+ loss was only 0.7%.

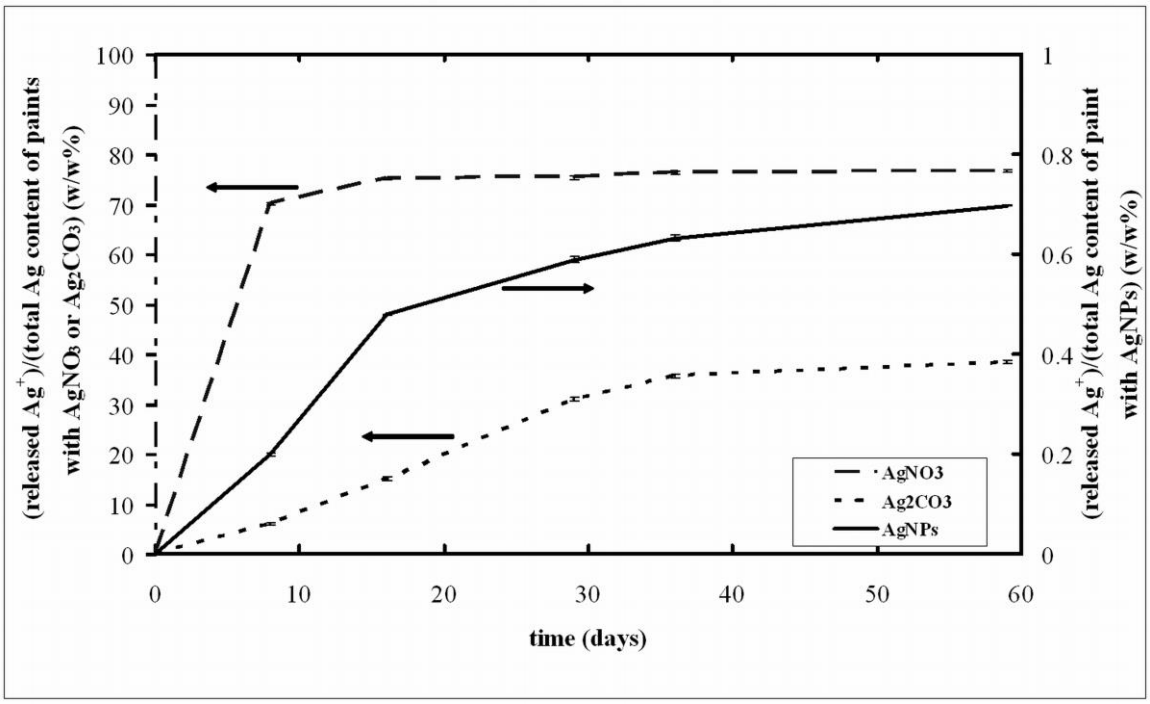

Fig. 7. Ratio (%) of released Ag^+ to the total Ag content of different coatings, as a function of time. Left 'y' axis refers to paints with silve-nitrate (dashed line) and silver-carbonate (dotted line), right 'y' axis refers to paint with AgNPs@GMPs (continuous line).
>>Fig. 7., size: 1.0 column; greyscale on the web, greyscale in print<<

3.7. *Anti-fouling effectiveness of the coatings*

The fluorescent dye causes reddish colorization to biolayers, wherethrough with captured fluorescent micrographs it was possible to follow the actual state of biofilm coverage. Based on software-processed photographs, diagrams of Fig. 8 demonstrate the growth of biofilm on three different paint samples as a function of time. The inserted pictures taken at the 20th week show the actual spreading of biolayers in natural water. By the end of the 7-month-long experiment, the reference samples without any anti-foulant became almost totally covered by biofilm (Fig. 8,a). Ag_2CO_3- and AgNPs@GMPs-containing ship coatings had relevant inhibiting effect even in the 23th and 28th weeks (Fig. 8,b and c, respectively). It is important to note that though these two compositions had similar efficacy, by the 6th week the coating with AgNPs@GMPs had lost only 0.6% of its total silver content, while the other with Ag_2CO_3 had lost 40% (based on Fig. 7).

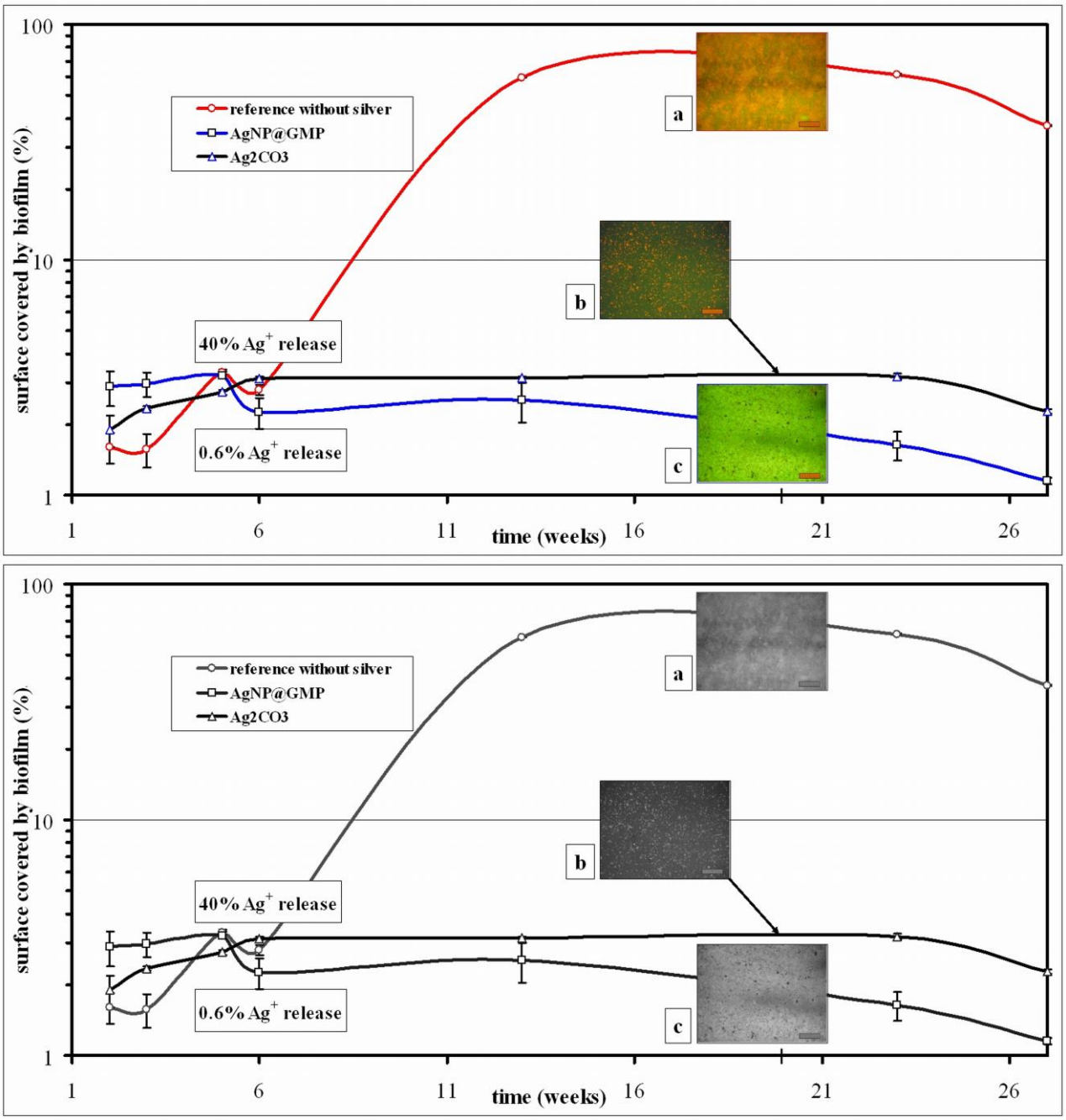

Fig. 8. Biofilm adhesion results: ratio of biofilm-covered area to total painted area (%, logarithmic scale) as a function of time. a, reference – without anti-foulant; b, with silver-carbonate; c, with encapsulated AgNPs. Reddish areas on the built-in fluorescence images represent the actual state of biofilm coverage after ~20 weeks.
>>Fig. 8., size: 1.5 column; color on the web, greyscale in print<<

4. Conclusion

On the basis of results it can be concluded that our novel, one-step w/o dispersion polymerization method is a proper way to obtain hardly swelling microparticles of peptide with *in situ* reduced, well-dispersed AgNPs. The advantage of this polymeric substance is its assistance in the proper reduction of silver. With the use of urea as co-monomer, the swelling was successfully blocked, thus the microparticles have an elongated release profile of the

active component. Based on the adhesion test, application of AgNPs@GMPs as additive in paints opens a prosperous future for antifouling coatings.
It was important for us to build microspheres from biocompatible materials. The only component in the reaction is the formaldehyde which is no bioacceptable, but it could be replaced by other, more eco-friendly chemicals.
This method and its product is, however, not limited to the coating technology. With certain changes in molar ratios and conditions, the reaction can result in softer or harder materials with tailored characteristics, for example with higher release ratio or swelling rate, thus the product could be applied in the medical field.

5. Acknowledgement

We acknowledge the work of the following colleagues who helped our work: Péter Németh, Eszter Drotár, László Szabó in electronmicroscopy, Zoltán Sándor in ICP measurements and Egrokorr Zrt providing the basic composition of an anti-fouling paint.

6. References

[1] Q. Li, S. Mahendra, D.Y. Lyon, L. Brunet, M.V. Liga, D. Li, P.J.J. Alvarez, Water Res. 42 (2008) 4591– 4602.
[2] N. Duran, P.D. Marcato, G.I.H. De Souza, O.L. Alves, E. Esposito, J. Biomed. Nanotechnol. 3 (2007) 203–208.
[3] S. Egger, R.P. Lehmann, M.J. Height, M.J. Loessner, M. Schuppler, Appl. Environ. Microbiol. 75 (2009) 2973–2976.
[4] M. Jasiorski, A. Leszkiewicz, S. Brzeziński, G. Bugla-Płaskońska, G. Malinowska, B. Borak, I. Karbownik, A. Baszczuk, W. Stręk, W. Doroszkiewicz, J. Sol-Gel Sci. Technol. 51 (2009) 330–334.
[5] B. Mahltig, D. Fiedler, A. Fischer, P. Simon, J. Sol-Gel Sci. Technol. 55 (2010) 269–277.
[6] M. Marini, S.D. Niederhausern, R. Iseppi, Biomacromolecules 8 (2007) 1246–1254.
[7] D. Lee, R.E. Cohen, M.F. Rubner, Langmuir 21 (2005) 9651–9659.
[8] Z. Li, D. Lee, X. Sheng, R.E. Cohen, M.F.Rubner, Langmuir 22 (2006) 9820–9823.
[9] D.W. Sheel, L.A. Brook, I.B. Ditta, P. Evans, H.A. Foster, A. Steele, Int. J. Photoenergy (2008) doi:10.1155/2008/168185.
[10] A. Kumar, K.V. Praveen, M.A. Pulickel, J. George, Nat. Mater. 7 (2008) 236-241.
[11] R.D. Holtz, B.A. Lima, A.G.S. Filho, M. Brocchi, O.L. Alves, Nanomed. Nanotechnol. Biol. Med. 8 (2012) 935-940.
[12] K. Naddafi, H. Jabbari, M. Chehrehei, Iran. J. Environ. Health Sci. Eng. 7 (2010) 223–228.
[13] M. Zielecka, E. Bujnowska, B. Kępska, M. Wenda, M. Piotrowska, Prog. Org. Coat. 72 (2011) 193-201.
[14] R. Kaegi, B. Sinnet, S. Zuleeg, H. Hagendorfer, E. Mueller, R. Vonbank, M. Boller, M. Burkhardt, Environ. Pollut. 158 (2010) 2900-2905.
[15] D.R Monteiro, L.F. Gorup, A.S. Takamiya, A.C. Ruvollo, E.R. de Camargo, D.B. Barbosa, Int. J. Antimicrob. Agents 34 (2009) 103–110.
[16] Y. Shinonaga, K. Arita, Acta Biomater. 8 (2012) 1388-1393.
[17] C. Bai, M. Liu, Nano Today 7 (2012) 258-281.
[18] S. Sutha, G. Karunakaran, V. Rajendran, Ceram. Int. (2013) http://dx.doi.org/10.1016/j.ceramint.2012.12.019

[19] N.A. Trujillo, R.A. Oldinski, H. Ma, J.D. Bryers, J.D. Williams, K.C. Popat, Mater. Sci. Eng., C 32 (2012) 2135-2144.
[20] P. Devasconcellos, S. Bose, H. Beyenal, A. Bandyopadhyay, L.G. Zirkle, Mater. Sci. Eng., C 32 (2012) 1112-1120.
[21] A. Simchi, E. Tamjid, F. Pishbin, A.R. Boccaccini, Nanomed. Nanotechnol. Biol. Med. 7 (2011) 22-39.
[22] K. Chaloupka, Y. Malam, A.M. Seifalian, Trends Biotechnol. 28 (2010) 580-588.
[23] B.S. Atiyeh, M. Costagliola, S.N. Hayek, S.A. Dibo, Burns 33 (2007) 139–148.
[24] D. Parsons, P.G. Bowler, V. Myles, S. Jones, Wounds 17 (2005) 222–232.
[25] P. Muangman, C. Chuntrasakul, S. Silthram, S. Suvanchote, R. Benjathanung, S. Kittidacha, S. Rueksomtawin, J. Med. Assoc. Thai 89 (2006) 953–958.
[26] Z. Jovanovic, J. Stojkovska, B. Obradovic, V. Miskovic-Stankovic, Mater. Chem. Phys. 133 (2012) 182-189.
[27] S. Saha, A. Pal, S. Kundu, S. Basu, T. Pal, Langmuir 26 (2010) 2885-2893.
[28] P. Rujitanaroj, N. Pimpha, P. Supaphol, Polymer 49 (2008) 4723–4732.
[29] X. Xu, M. Zhou, Fibers Polym. 9 (2008) 685–690.
[30] A. Yiwei, Y. Yunxia, Y. Shuanglong, D. Lihua, D. Guorong, Mater. Chem. Phys. 104 (2007) 158–161.
[31] M. Darroudi, M.B. Ahmad, A.H. Abdullah, N.A. Ibrahim, K. Shameli, Int. J. Mol. Sci. 11 (2010) 3898-3905.
[32] M.B. Ahmad, J.J. Lim, K. Shameli, N.A. Ibrahim, M.Y. Tay, Molecules 16 (2011) 7237-7248.
[33] M. Darroudi, M.B. Ahmad, A.K. Zak, R. Zamiri, M. Hakimi, Int. J. Mol. Sci. 12 (2011) 6346-6356.
[34] M.B. Ahmad, J.J.L. Lim, K. Shameli, N.A. Ibrahim, M.Y. Tay, B.W. Chieng, Chem. Cent. J. 6 (2012) 101.
[35] V. Rattanaruengsrikul, N. Pimpha, P. Supaphol, J. Appl. Polym. Sci. 124 (2012) 1668–1682.
[36] Q. Wu, H. Cao, Q. Luan, J. Zhang, Z. Wang, J.H. Warner, A.A.R. Watt, Inorg. Chem. 47 (2008) 5882–5888.
[37] J.J. Martin, J.M. Cardamone, P.L. Irwin, E.M. Brown, Colloids Surf., B 88 (2011) 354-361.
[38] A. Travan, C. Pelillo, I. Donati, E. Marsich, M. Benincasa, T. Scarpa, S. Semeraro, G. Turco, R. Gennaro, S. Paoletti, Biomacromolecules 10 (2009) 1429–1435.
[39] A. Pal, K.J. Esumi, J. Nanosci. Nanotechnol. 7 (2007) 2110–2115.
[40] S. Saha, A. Pal, S. Pande, S. Sarkar, S. Panigrahi, T. Pal, J. Phys. Chem. C 113 (2009) 7553-7560.
[41] Y. Liu, S. Chen, L. Zhong, G. Wu, Radiat. Phys. Chem. 78 (2009) 251–255.
[42] S. Chen, G. Wu, H. Zeng, Carbohydr. Polym. 60 (2005) 33–38.
[43] P. Sanpui, A. Murugadoss, P.V.D. Prasad, S.S. Ghosh, A. Chattopadhyay, Int. J. Food Microbiol. 124 (2008) 142–146.
[44] S. Lu, W. Gao, H.Y. Gu, Burns 34 (2008) 623–628.
[45] A. Murugadoss, A. Chattopadhyay, Nanotechnology 19 (2008) 015603/1-015603/9.
[46] R. Yoksan, S. Chirachanchai, Mater. Chem. Phys. 115 (2009) 296–302.
[47] W.-L. Du, S.-S. Niu, Y.-L. Xu, Z.-R. Xu, C.-L. Fan, Carbohydr. Polym. 75 (2009) 385–389.
[48] P. Raveendran, J. Fu, S.L. Wallen, Green Chem. 8 (2005) 34–38.
[49] V. Thomas, M. Namdeo, Y.M. Mohan, S.K. Bajpai, M. Bajpai, J. Macromol. Sci., Part A Pure Appl. Chem. 45 (2008) 107–119.
[50] V.K. Sharma, R.A. Yngard, Y. Lin, Adv. Colloid Interface Sci. 145 (2009) 83–96.

[51] Y. Park, Y.N. Hong, A. Weyers, Y.S. Kim, R.J. Linhardt, IET Nanobiotechnol. 5 (2011) 69–78.
[52] M. Darroudi, M.B. Ahmad, A.H. Abdullah, N.A. Ibrahim, Int. J. Nanomed. 6 (2011) 569–574.
[53] T. Szabó, L. Molnár-Nagy, J. Bognár, L. Nyikos, J. Telegdi, Prog. Org. Coat. 72 (2011) 52-57.
[54] J.H. Muyonga, C.G.B. Cole, K.G. Duodu, Food Chem. 86 (2004) 325-332.
[55] S. Farris, J. Song, Q. Huang, J. Agric. Food Chem. 58 (2010) 998–1003.